Journal of Catalysis **181,** 80–90 (1999)
Article ID jcat.1998.2217, available online at http://www.idealibrary.com on IDEAL®

Study of Cesium or Cesium-Transition Metal-Substituted Keggin-Type Phosphomolybdic Acid as Isobutane Oxidation Catalysts

I. Structural Characterization

M. Langpape,* J. M. M. Millet,* U. S. Ozkan,† and M. Boudeulle‡

*Institut de Recherches sur la Catalyse, CNRS, associé a l'Université Claude-Bernard, Lyon I, 2 avenue A. Einstein, F-69626 Villeurbanne Cedex, France; †Department of Chemical Engineering, Ohio State University, 140 West 19th Avenue, Columbus, Ohio 43210; ‡Laboratoire de Physico-Chimie des Matériaux Muminescents, Université Claude-Bernard Lyon I, 17 boulevard du 11 novembre 1918, F-69626 Villeurbanne Cedex, France

Received March 4, 1998; revised June 16, 1998; accepted June 16, 1998

Cesium and cesium-transition metal-substituted Keggin-type phosphomolybdic acids have been prepared and characterized using several techniques. The results obtained show that all heteropolycompounds with formulae $H_{3-x}Cs_xPMo_{12}O_{40}$, where $0 < x < 3$ were composed of two phases corresponding to the hydrated acid and the pure cesium salt with the acid phase coating the salt particles. For compounds with $x < 2$, the acid was present in large amounts and could be detected by X-ray diffraction. For compounds with $x > 2$ the precipitation rates vary, leading to very small cesium salt particles. In this second case the acid phase also coated the particles, but it was no longer detectable by X-ray diffraction, although it could be observed by XPS or Raman spectroscopy. All the data obtained show that the transition metal cations are replacing the protons in the supported acid phase and not the cesium atoms in the salt. This replacement does not change the structure of the bulk acid phase even at high substitution levels, but it decreases the hydration rate of the supported acid.

1. INTRODUCTION

The potential use of alkaline and transition metal-substituted $H_3PMo_{12}O_{40}$ compounds as catalysts in the oxidation of alkanes has recently been reported (1–2). These compounds have been shown to oxidize ethane, propane, and butane (3–6), but the more remarkable results have been obtained when they were used as catalysts to partially oxidize isobutane into methacrylic acid (7–9). The heteropolycompounds studied for this reaction are complex; both alkaline and transition metals substituting partially or totally the protons of the acid. Compounds with the general formula $Cs_{2.5}M_x^{y+}H_{0.5-xy}PMo_{12}O_{40}$ with $M =$ Mn, Fe, Co, Ni, Cu have been shown to be very efficient catalysts with an optimal activity obtained with 0.08 Ni^{2+} and the highest selectivity to methacrylic acid with 0.08 Ni^{2+} or 0.08 Fe^{3+} (7).

Two models for the structure of alkaline metal-substituted heteropolyacids have been proposed in the literature. In the first one, the acidic alkaline salts consist of a surface layer of $H_3PMo_{12}O_{40}$ dispersed on the particle of $A_3PMo_{12}O_{40}$ (10, 11). In the second model a solid solution of the form $A_{3-x}H_xPMo_{12}O_{40}$ is proposed. In this last case, however, the authors report that the solid solution was formed upon heating and that the two phases cited above should coexist in the samples synthesized at room temperature (12). The effect of the co-substitution of a transition metal, together with alkaline metals on the structural and physicochemical characteristics of the heteropolyacids has never been studied.

In this paper we present a detailed characterization of cesium and cesium-transition metal-substituted phosphomolybdic acids with two objectives: (1) to contribute to the overall understanding of the structure of the alkaline metal-substituted heteropolyacids and resolve the controversies, (2) to determine the effect of the co-substitution of transition metal both on the structure and on the physicochemical properties. In order to achieve these goals two series of heteropolycompounds of general formula $Cs_xH_{3-x}PMo_{12}O_{40}$ with $0 \le x \le 3$ and $Cs_2M_x^{y+}H_{3-yx}PMo_{12}O_{40}$ with $M =$ Fe or Cu and $0 \le x \le 0.3$ have been prepared and characterized. An heteropolyacid substituted only with iron, $Fe_{0.85}H_{0.45}PMo_{12}O_{40}$, has also been studied.

2. EXPERIMENTAL

2.1. Preparation of the Samples

Cesium-substituted heteropolycompounds have been synthesized by dropwise addition of an aqueous solution of Cs_2CO_3 (0.08 *M*) to an aqueous solution of $H_3PMo_{12}O_{40}$ (0.06 *M*) at 323 K and in the desired stoichiometry. The pure acid $H_3PMo_{12}O_{40}$ has been prepared using a well-established procedure (13). After evaporating the water at reduced pressure at 323 K, the precipitate was calcined for 5 h at 623 K under an air flow. The iron- and

0021-9517/99 $30.00

copper-containing salts were prepared using the same protocol, the transition metal being added to the acid as an aqueous solution of its nitrate before the addition of the Cs_2CO_3 solution. The $Fe_{0.85}H_{0.45}PMo_{12}O_{40}$ compound was prepared by crystallization from a concentrated solution containing the pure acid and iron nitrate in a 1 : 1 stoichiometry. The crystals obtained were dried in air and calcined as described above. The prepared solids were generally stored in air at room temperature. In these conditions they were rapidly rehydrated as shown in the results section. They are designated according to their metal countercation content. For example, $Cs_2Fe_{0.2}$ denotes a solid with the stoichiometry $Cs_2Fe_{0.2}H_{0.4}PMo_{12}O_{40}$.

2.2. Characterization Techniques

Chemical analysis was determined by atomic emission for Mo, Cu, Fe, and P, using an induced plasma technique, and for Cs, using an air–acetylene flame. The specific surface areas were determined by the BET method using nitrogen adsorption at 77 K. The infrared spectra were measured as KBr pellets on a Brucker Vector 22 FTIR spectrometer. Raman spectra were recorded at room temperature using a DILOR XY spectrophotometer equipped with an intensified photodiode array detector. The emission line at 514.5 nm from an Ar^+ ion laser (Spectra Physics, Model 2016) was used for excitation at low power (about 1 mW). The resolution was about 1 cm^{-1}.

X-ray diffraction patterns were recorded using a Siemens D500 diffractometer and Cu$K\alpha$ radiation. A refinement program has been used to calculate the unit cell parameters of the samples (14). Electron microscopy, coupled with EDX analysis, was performed with a conventional transmission electron microscopy (JEOL JEM 2010 (200 kV)) in a high resolution configuration (resolution picture point: 0.194 nm), equipped with an energy dispersive X-ray spectrometer (PENTAFET detector + LINK ISIS analyzer system). A dry dispersion of the finely grounded powder was used to prepare the samples in order to avoid any dissolution of the heteropolyacid.

TGA experiments were performed under a nitrogen flow (1.2 $dm^3 \cdot h^{-1}$) using a SETARAM TGA-DTA 92 thermobalance with about 30 mg of product and a heating rate of 5 $K \cdot min^{-1}$. XPS measurements were performed with a VG ESCALAB 200 R. Binding energies were corrected relative to the carbon 1S signal at 284.6 eV. Quantitative analysis of the peaks, in terms of elemental ratios, was carried out as described previously (15) and the experimental precision on XPS quantitative measurements was considered to be around 10%.

Isopropyl alcohol (IPA) decomposition tests were carried out in a quartz fixed-bed reactor fed by a 3% IPA in air (total flow = 30 $cm^3 \cdot min^{-1}$) in the temperature range 353–393 K. A gas chromatograph equipped with both flame ionization and thermal conductivity detectors was used to analyze the products. The samples were preheated for 1 h at 573 K in flowing air in each experiment before the IPA/air mixture was fed.

3. RESULTS

3.1. Chemical Analyses, Thermogravimetric Analyses and BET Surface Area Measurements

The chemical and thermogravimetric analyses data are presented in Table 1. The results of chemical analyses were in good agreement with the desired stoichiometries. It was noticed that preparing the pure cesium salt with the method described above always results in a solid containing a small but nonnegligible amount of acid ($Cs_{2.88}H_{0.12}$). The TG curves showed the two previously reported features attributed to crystal water loss up to 523 K and constitutional water loss between about 523 and 623 K (16) (Fig. 1a). The two water losses were well separated in the case of the pure acid, but they began to overlap for mixed salts, especially for those with a high content of cesium countercations. The pure acid showed a degree of hydration of 13 molecules of water per Keggin unit (KU) with slight intermediate stabilizations at about 8 and 3 molecules, according to literature (17). Mixed salts were considered as composed of a dry cesium salt and a hydrated acid phase, according to results described later in this article. Cs_1H_2 showed a hydration level (based on per mole of acid) close to that of the pure acid. The Cs_2H_1 and $Cs_{2.5}H_{0.5}$ compounds were found to contain less water than those with lower cesium contents

TABLE 1

Chemical Analyses and Thermogravimetric Analyses Data

	Atomic ratios			Hydration water loss	
Compound	12 Cs/Mo	12 M/Mo	Mo/P	/KU	/KU of acid
H_3	—	—	11.7	13	13
Cs_1H_2	1.0	—	11.3	5	9
$Cs_{1.5}H_{1.5}$	1.5	—	11.6		
Cs_2H_1	2.0	—	11.7	2	7
$Cs_{2.5}H_{0.5}$	2.40	—	11.5	1	6
Cs_3	2.86	—	11.3		
$Cs_2Fe_{0.05}$	1.8	0.05	11.4	0.7	2.2
$Cs_2Fe_{0.10}$	1.8	0.10	11.4	0.7	2.1
$Cs_2Fe_{0.20}$	1.8	0.21	11.8	1.5	4.5
$Cs_2Fe_{0.25}$	1.8	0.25	11.6	0.8	2.5
$Cs_2Fe_{0.30}$	1.8	0.31	11.5	1.6	4.7
$Fe_{0.85}H_{0.45}$	—	0.85	11.4	13	13
$Cs_2Cu_{0.05}$	1.9	0.06	11.1	1	3
$Cs_2Cu_{0.10}$	1.9	0.11	11.1	1.3	3.8
$Cs_2Cu_{0.20}$	1.9	0.22	11.1	0.8	2.4
$Cs_2Cu_{0.30}$	1.8	0.32	11.0	1.5	4.6
$Cs_2Cu_{0.43}$	1.8	0.42	11.3	0.8	2.5

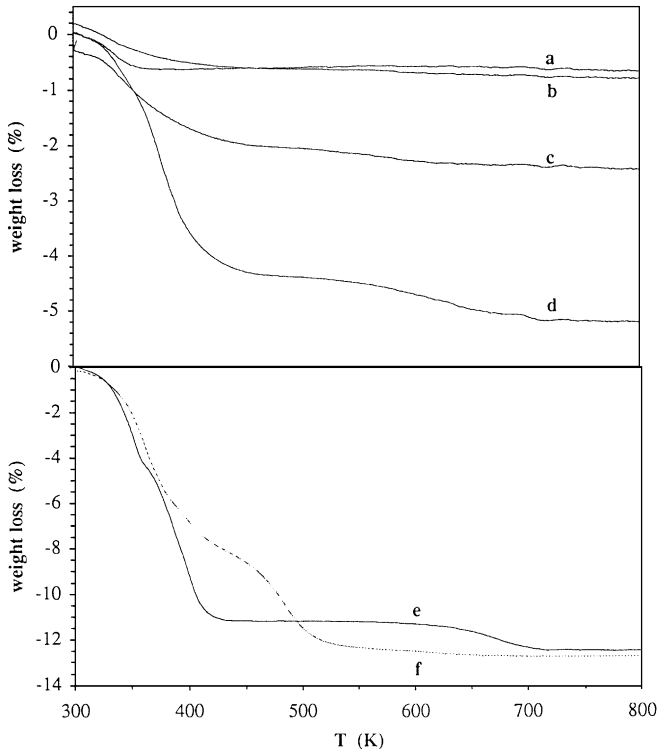

FIG. 1. Thermogravimetric profiles of the compounds dried in air: (a) Cs_3; (b) $Cs_{2.5}H_{0.5}$; (c), Cs_2H_1; (d) Cs_1H_2; (e) acid; (f) $Fe_{0.85}H_{0.45}$.

(6 to 7 moles as opposed to 13 moles of water per mole of acid 13) (Fig. 1). The thermogravimetric analysis of the pure acid dried for two weeks at room temperature over silica gel showed a crystal water content of only 8 molecules per KU for this sample. The similar treatment applied to a Cs_1H_2 sample also led to the same reduced water content. The end of the hydration water loss was systematically observed at a higher temperature (523 K) for cesium-containing compounds than for pure acid (423 K).

The addition of iron or copper to Cs_2H_1 modified the water content of the solids and to a lesser extent their thermal behavior (Table 1). For the Cs_2Fe_x and Cs_2Cu_x compounds the water loss is lower than that of the undoped Cs_2H_1 with 2 to 5 water molecules per mole of acid instead of 7. The extent of hydration did not seem to vary with the relative transition metal content, but rather with the conditions under which the solids were stored. The second water loss could not be resolved from the first one. Finally, the analysis of the $Fe_{0.85}H_{0.45}$ sample showed that it was similar to the pure acid hydrated with 13 water molecules (Fig. 1b). Nevertheless the end of hydration water loss occurred at 523 K, instead of 425 K, for the pure acid and the stabilization of an intermediate state at 5 moles of water per KU was clearly visible. The specific surface areas of the solids increased with their cesium content (Fig. 2a); such behavior has already been reported and related to the change in morphology corresponding to the formation of small spherical-shaped particles obtained by precipitation (11, 18, 19). Figure 2b shows that the specific surface areas of the Cs_2H_x samples increased with the Fe^{3+} content, whereas they remained practically unchanged with the Cu^{2+} content. Since the cesium content in these samples was kept constant, the additional change in surface area is due to the incorporation of a transition metal and this effect appears to be specific to the transition metal ion (i.e., iron vs copper) on the surface.

3.2. X-Ray Diffraction Analysis

The X-ray diffraction analysis results obtained on the Cs_xH_{3-x} compounds are presented in Tables 2 and 3 and illustrated in Figs. 3 and 4. Figure 3 shows the X-ray diffraction patterns of the compounds of the Cs_xH_{3-x} series stored at ambient conditions. The pure acid had the triclinic (P-1) phase corresponding to the hydrate with 13 water molecules

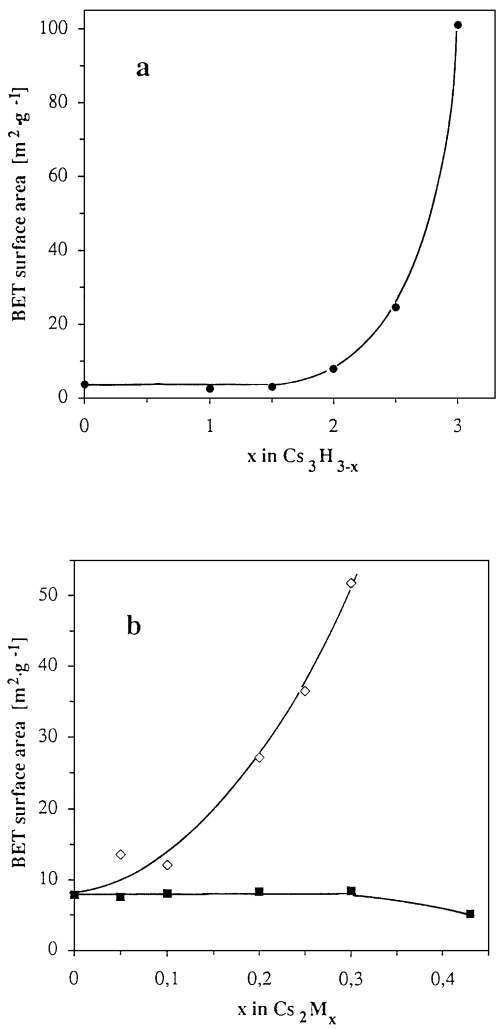

FIG. 2. Variation of the specific surface area of (a) the Cs_xH_{3-x} compounds as a function of the cesium content, (b) the Cs_2M_x compounds as a function of the Cu (■) and Fe (◇) content.

TABLE 2

Calculated Cell Parameter of the Cubic Phase in the Cesium and Iron or Copper Substituted Compounds

Compound	a (Å)	Compound	a (Å)	Compound	a (Å)
Cs_1H_2	11.819(8)				
$Cs_{1.5}H_{1.5}$	11.805(6)	$Cs_2Fe_{0.05}$	11.804(11)	$Cs_2Cu_{0.05}$	11.813(4)
Cs_2H_1	11.820(7)	$Cs_2Fe_{0.10}$	11.805(13)	$Cs_2Cu_{0.10}$	11.817(6)
$Cs_{2.5}H_{0.5}$	11.825(5)	$Cs_2Fe_{0.20}$	11.810(10)	$Cs_2Cu_{0.20}$	11.818(4)
Cs_3	11.828(6)	$Cs_2Fe_{0.30}$	11.818(12)	$Cs_2Cu_{0.30}$	11.819(7)

per KU (20). When protons were partially substituted by cesium cations, a new phase was formed which corresponds to a cubic (Pn3m) phase commonly associated with the pure alkaline heteropolysalts (21). For salts with less than two cesium atoms per KU both phases were observed, whereas only the cubic phase was formed for salts with more than two cesium atoms. Such observation has previously been reported (11). The cell parameters of the cubic phase have been calculated for the different solids of the series (Table 2); they did not vary significantly with the cesium content of the heteropolycompounds. In the same way the

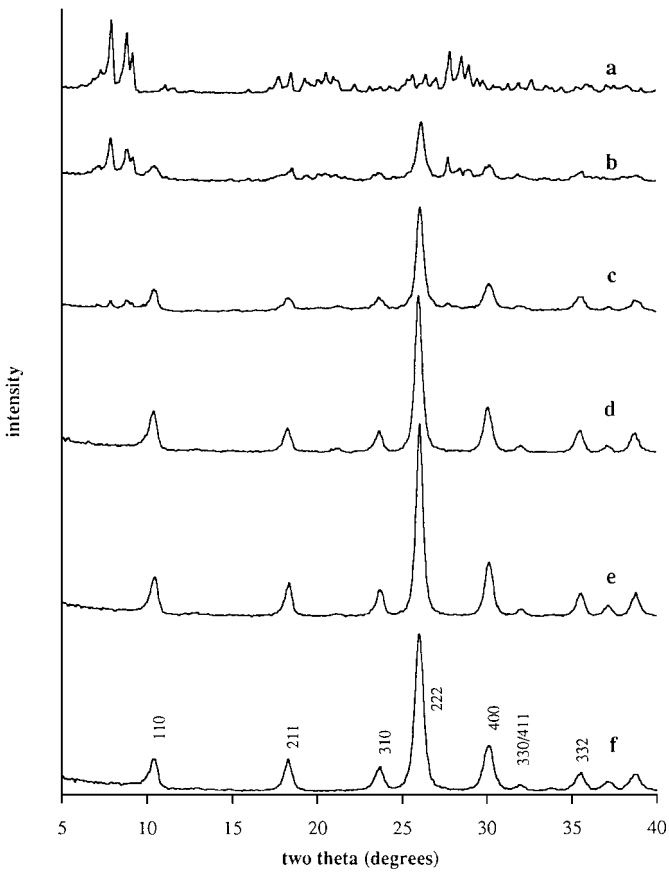

FIG. 3. X-ray diffraction patterns of the Cs_xH_{3-x} compounds: (a) H_3; (b) Cs_1H_2; (c) $Cs_{1.5}H_{1.5}$; (d) Cs_2H_1; (e) $Cs_{2.5}H_{0.5}$; (f) Cs_3.

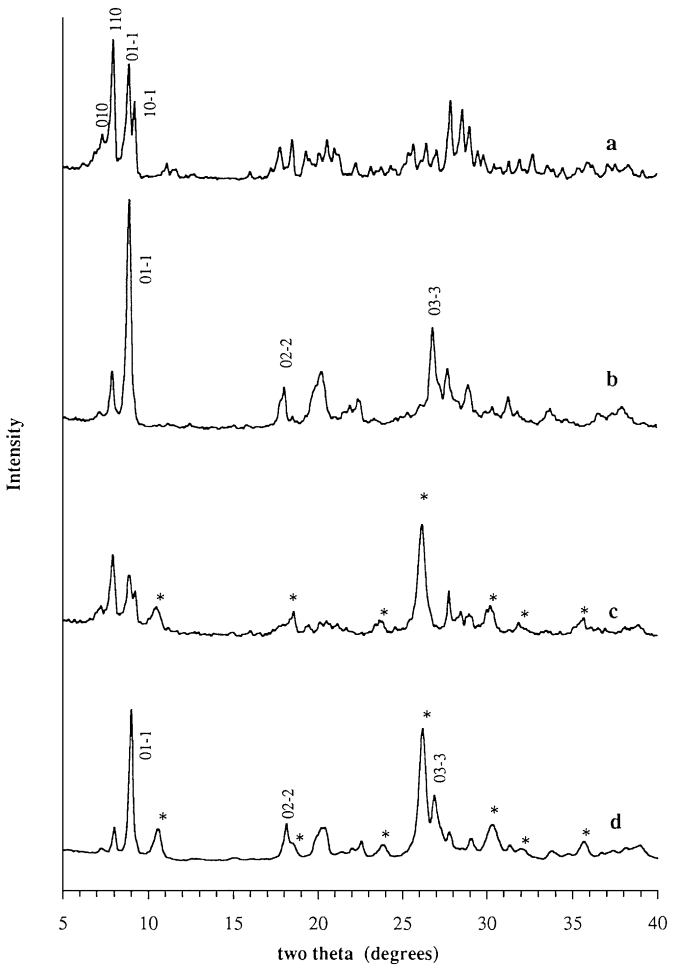

FIG. 4. X-ray diffraction patterns of (a) the pure acid dried in air, (b) the pure acid dried for two weeks at room temperature over silica gel, (c) the Cs_1H_2 dried in air, (d) the Cs_1H_2 dried for two weeks at room temperature over silica gel. ∗ denotes the peaks of the cesium salt cubic structure.

triclinic cell parameters were comparable for the acid phase and for the Cs_1H_2 compound (Table 3). The acid and Cs_1H_2 compounds, which showed a crystal water content of only eight molecules per KU of acid after drying for about two weeks at room temperature over silica gel, showed modified X-ray patterns (Fig. 4). These patterns were similar to that previously reported by Black *et al.* for an acid phase

TABLE 3

Comparison of the Cell Parameters of the Triclinic Phase of the Hydrated Acid Phase (13 H_2O), Detected in the Pure Acid (H_3), in the Cs_1H_2 Compound and in the Iron-Doped Acid ($Fe_{0.85}H_{0.45}$)

Compound	a	b (Å)	c	α	β (°)	γ
H_3	14.54(11)	14.79(12)	13.65(8)	114.0(6)	111.7(4)	59.0(6)
Cs_1H_2	14.54(11)	14.78(13)	13.64(9)	113.9(7)	111.7(4)	58.9(5)
$Fe_{0.85}H_{0.45}$	14.55(11)	14.81(12)	13.68(10)	114.2(6)	111.8(4)	59.0(4)

hydrated at about 8 H_2O and described as a new phase (11). But a comparison of these patterns with that of the 13 H_2O-acid triclinic form showed a strong similarity. The (0, k, −k) reflections were the same for the 13-H_2O and 8-H_2O containing forms of the hydrated acid, with the relative intensity of these peaks being higher for the samples containing eight water molecules (Figs. 4a and c) than for the samples containing 13 water molecules (Figs. 4b and d). No other structure seemed correspond to these patterns. The X-ray diffraction patterns of Cs_2Cu_x and Cs_2Fe_x compounds exhibited only the cubic phase without any change in the cell parameters with the transition metal content of the heteropolycompounds (Table 2). The $Fe_{0.85}H_{0.45}$ sample was found to crystallize with the triclinic 13 H_2O acid structure and showed cell parameters close to those of the pure acid phase (Table 3).

3.3. *Infrared and Raman Spectroscopies*

The comparison of the IR spectra of the compounds did not reveal significant differences. Within the range 1100–600 cm^{-1}, the bands corresponding to the stretching of the Mo-O bonds in the Keggin unit were observed with approximately the same wave-numbers. The study of the solids using Raman spectroscopy has been focused on the same frequency range. The Raman spectra of the Cs_xH_{3-x} compounds are shown on Fig. 5. The corresponding band assignments are presented in Table 4. All the spectra obtained showed the bands corresponding to the ν_s Mo=O_t (991 cm^{-1}), ν_{as} Mo=O_t (974 cm^{-1}), ν_s P-O_p (961 cm^{-1}), and ν_{as} Mo-O_b-Mo (878 cm^{-1}) vibrations as observed in the potassium salt (22, 23) and bands at 1009, 1002, and 860 cm^{-1} which can be attributed to the pure acid phase (23). Since differences in energies and relative intensities were observed for the bands, specially for those in the range of 860–930 and 990–1020 cm^{-1}, we have performed a multiband fit of the spectra. These fits revealed that the band at 991 cm^{-1} was relatively asymmetric and that two bands at 991 and 986 cm^{-1} had to be considered in order to get good fits. Both of these bands, which can be observed in all of the spectra with approximately the same relative intensities, have been attributed to the ν_sMo=O_t vibration in the cesium salt. The high frequency of these bands should be due to the strong p character of the bond which is the shortest in the structure. The existence of the corresponding two bands has already been observed in the infrared spectra of other heteropolycompounds, but not been interpreted (23). The band at 1002 cm^{-1}, which showed a relative intensity decreasing with the cesium content, has been attributed to the same ν_sMo=O_t vibration but in the acid phase. The band around 1009 cm^{-1}, only observed in the spectra of the compounds with less than two cesium atoms per formula, has also been attributed to the acid phase but dehydrated or less hydrated. This assignment is based on the observation that the spectrum of the pure acid phase dehydrated at 623 K showed mainly the band at 1009 cm^{-1}, whereas that of the hydrated acid (13 H_2O) showed the band at 1002 cm^{-1} with the greater intensity. It can be noted that a similar band position shift had previously been reported comparing the spectra of anhydrous and hydrated phosphotungstic acids (23). An equivalent observation can be made concerning the ν_{as}Mo-O_b-Mo vibration which we observed at 880 cm^{-1} in the pure cesium salt and at 910 cm^{-1} in the acid phase. However, in this case the band at 880 cm^{-1} was still present in the spectrum of the pure acid. The substitution of protons by iron has been studied by Raman spectroscopy and the spectra of the compounds $Cs_2Fe_{0.2}$, $Cs_1Fe_{0.2}$, and $Fe_{0.85}H_{0.45}$ have been recorded (Fig. 6). They did not differ from those of the Cs_xH_{3-x} compounds with bands at the same positions except a new band at 933 cm^{-1} observed in the spectrum of $Fe_{0.85}H_{0.45}$. This band has been attributed to Fe-OH vibrations. Finally, it can be noted that Raman spectroscopy data never really showed the presence of molybdenum oxide after calcination at 623 K under air, except possibly for the Cs_1H_2 sample; molybdenum oxide is mainly characterized by a band at 820 cm^{-1} for the α form and two bands at 780 and 850 cm^{-1} for the β form (24). It was thus confirmed that the Keggin unit remained intact after the heat treatment at 613 K.

TABLE 4

Assignment of the Bands in the Raman Spectra in the 1100 to 800 cm^{-1} Region

Compound	Frequencies (cm^{-1})							
	ν_s Mo-O_t				ν_{as} Mo-O_t	ν_s P-O_p	ν_s Mo-O_b-Mo	
H_3	1012	1000					910	891
Cs_1H_2	1010	1002	991	984	975	963	912	880
$Cs_{1.5}H_{1.5}$	1009	1002	991	984	974	962	905	878
Cs_2H_1		1002	992	987	974	962		880
$Cs_{2.5}H_{0.5}$		1002	992	986	975	962		879
Cs_3		997	991	986	974	961		878

3.4. *Surface Chemical Analysis*

The XPS technique was used to characterize the mixed cesium salts without transition metal cations and those containing copper. The superposition of the CsKα3 and CsKα4 peaks with the Fe2p3/2 peak did not allow us to study the samples containing iron, the latter being present in very small amounts. The characterization was carried out after calcination and the results obtained are presented in Table 5. For the Cs_xH_{3-x} compounds, it could be observed that the surface Cs/Mo ratio was consistently lower than the one determined by chemical analysis. The same observation was made for the Cs_2Cu_x compounds, but in this case the surface Cu/Mo ratio was greater than that of the chemical analysis. All the compounds exhibited a Mo/P ratio close to 9 instead of 12. Such discrepancy between the surface

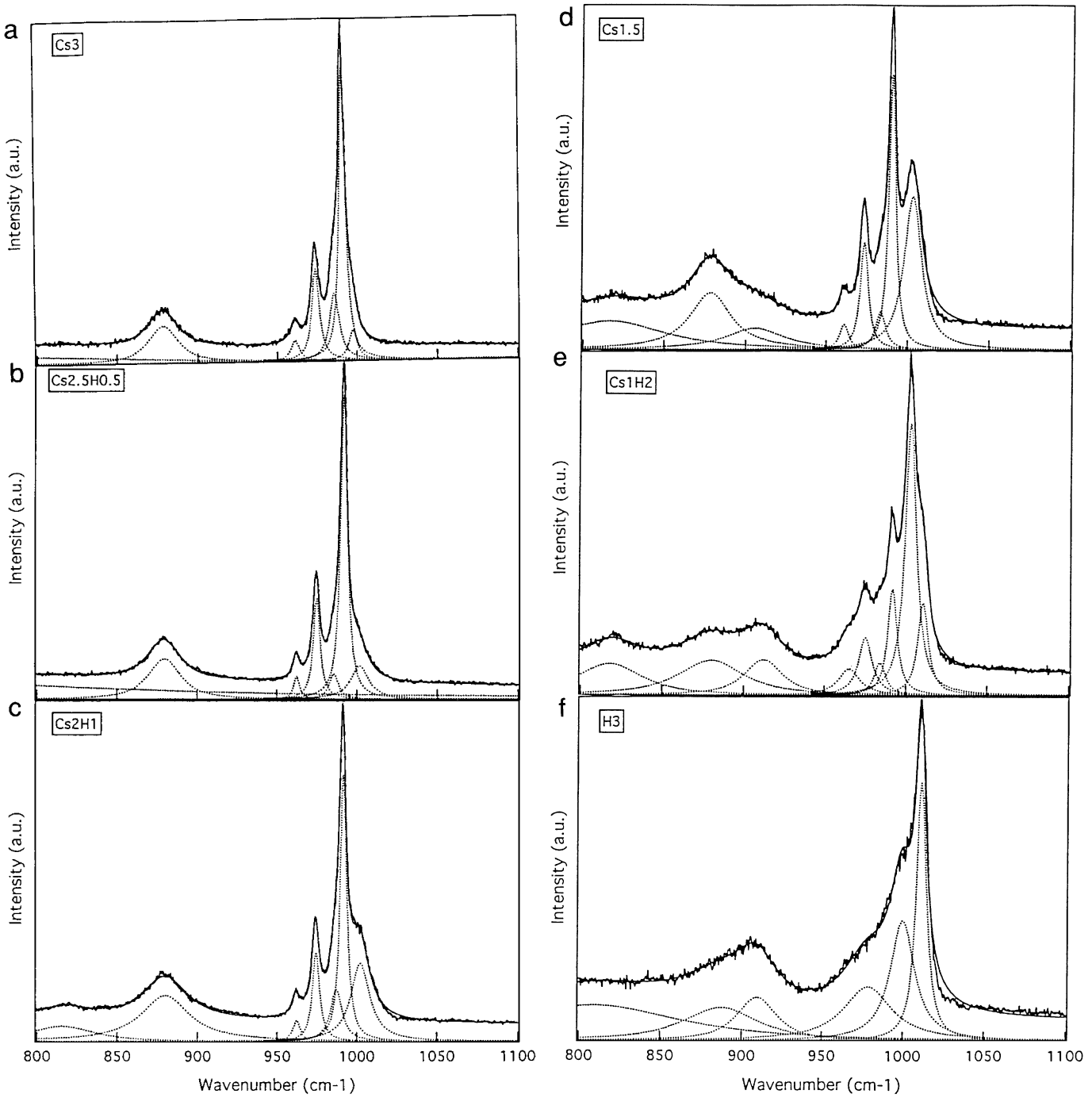

FIG. 5. Raman spectra of the Cs_xH_{3-x} compounds: (a) Cs_3; (b) $Cs_{2.5}H_{0.5}$; (c) Cs_2H_1; (d) $Cs_{1.5}H_{1.5}$; (e) Cs_1H_2; (f) H_3.

experimental and theoretical phosphorus composition in the case of VPO catalysts have been reported and are still debated (25, 26). The binding energies for the P_{2p} (134.1 eV) and $Mo_{3d5/2}$ (233.0 eV) peaks were characteristic of P^{5+} and Mo^{6+} cations, whereas the binding energy for the $Cu_{2p3/2}$ (933 eV) peak corresponded to Cu^+ cations. This assignment was confirmed by the absence of a peak at 940 eV, which is systematically present for Cu^{2+}.

3.5. Electron Microscopy

The study has been focused on the samples Cs_1H_2, Cs_2H_1 (Fig. 7) and $Cs_2Fe_{0.2}$ (Table 6). The Cs_1H_2 sample shows particles with a size of 50 to 600 nm, which appear to be embedded in a phase exhibiting a lower contrast in the micrographs (Fig. 7a). The EDX analysis performed over the particles showed a higher cesium content, with a Cs/Mo

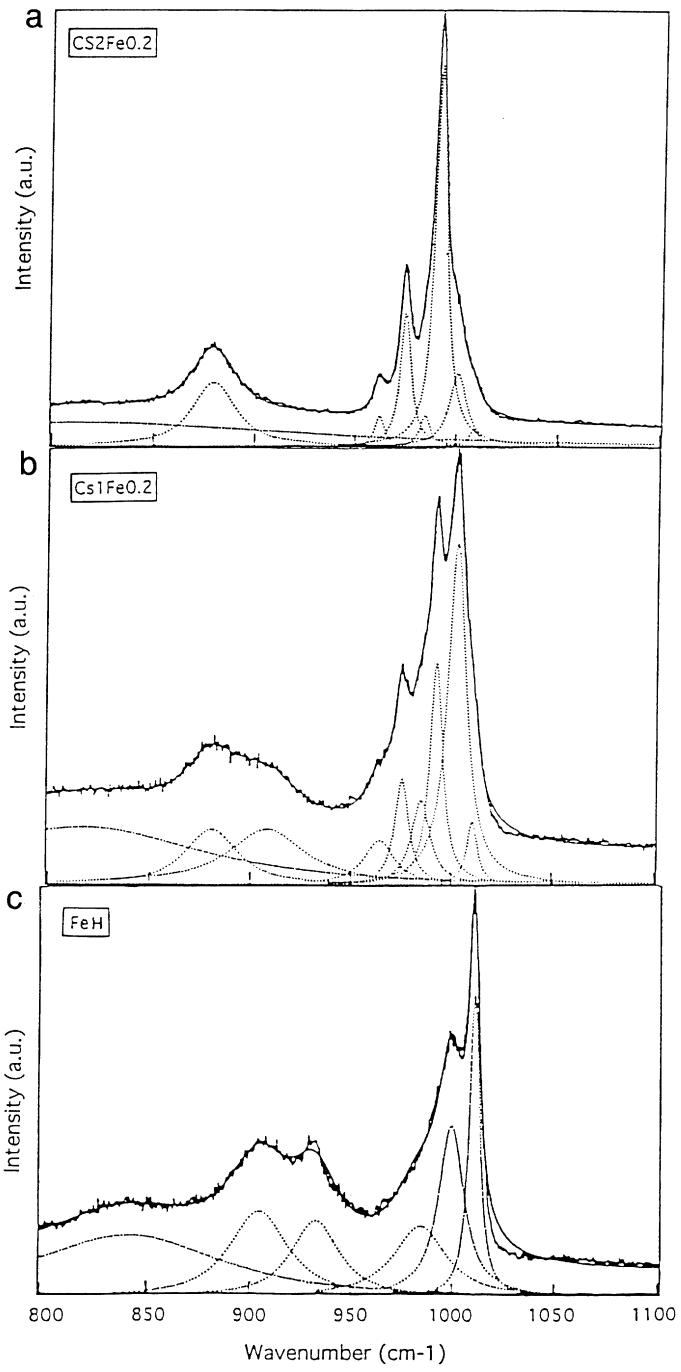

FIG. 6. Raman spectra of the iron containing compounds: (a) $Cs_2Fe_{0.2}$; (b) $Cs_1Fe_{0.2}$; (c) $Fe_{0.85}H_{0.45}$.

ratio close to that given by the chemical analysis whereas the surface phase contained practically no cesium (Table 6). The micrographs of the Cs_2H_1 sample (Fig. 7b) did not show the same morphology that was observed in Cs_1H_2 and only well contrasted spherical particles of 10 to 100-nm diameter were observed. The EDX analysis of these particles at the center and near the edge showed a lower Cs content on the near the surface (Table 6). The sample containing iron,

TABLE 5

Atomic Surface Composition of the Solids Calculated from XPS Analyses Data

Compound	Atomic ratios		
	Mo/P	12 Cs/Mo	12 Cu/Mo
H_3	8.5		
Cs_1H_2	8.6	0.5	
$Cs_{1.5}H_{1.5}$	10.2	1.0	
Cs_2H_1	8.9	1.7	
Cs_3	8.8	3.3	
$Cs_2Cu_{0.2}$	7.8	1.5	0.26
$Cs_2Cu_{0.3}$	7.7	1.4	0.49

$Cs_2Fe_{0.2}$, showed no significant differences as compared to the Cs_2H_1 compound. The particles showed the same lower Cs content near the edge. The lower cesium content near the edges was also accompanied by a higher iron conten. Regardless of the Cs or transition metal content observed, the molybdenum to phosphorus ratio appeared to remain stable with the expected value of 12 in every region analyzed.

3.6. Isopropyl Decomposition

The results from the catalytic decomposition of isopropyl alcohol (IPA) on Cs_xH_{3-x} compounds at 373 and 353 K are shown in Table 7. Over all of the compounds studied, we observed the formation of propene, di-isopropylether (DIPE), and acetone; no CO_2 was detected in the product mixture. The results are presented as observed formation rates using two different bases, namely per unit surface area and per gram of acid phase. It can be seen that the activity of the Cs_xH_{3-x} compounds decreased with increasing cesium content. There was a major drop in activity from Cs_1H_2 to Cs_2H_1 (almost a 10-fold decrease). The conversion rate over the Cs salt was very low. The product distibution over the acid containing compounds did not show major changes,

TABLE 6

EDX-STEM Analyses of Particles of Samples Cs_1H_2 (Fig. 7a), Cs_2H_1 (Fig. 7b), and $Cs_2Fe_{0.20}$

Compound		Analyzed area	12 Cs/Mo	Mo/P	12 Fe/Mo
Cs_1H_2	1	Whole particle	1.3	13	
	2	Whole small particle	1.1	12	
	3	Particle with low contrast	0.2	10	
	4	Particle with low contrast	0.5	12	
Cs_2H_1	1	Whole particle	2.1	13	
	2	Particle border	1.4	12	
	3	Particle border	1.5	12	
$Cs_2Fe_{0.2}$		Whole particle	2.3	12	0.20
		Particle border	1.6	11	0.33

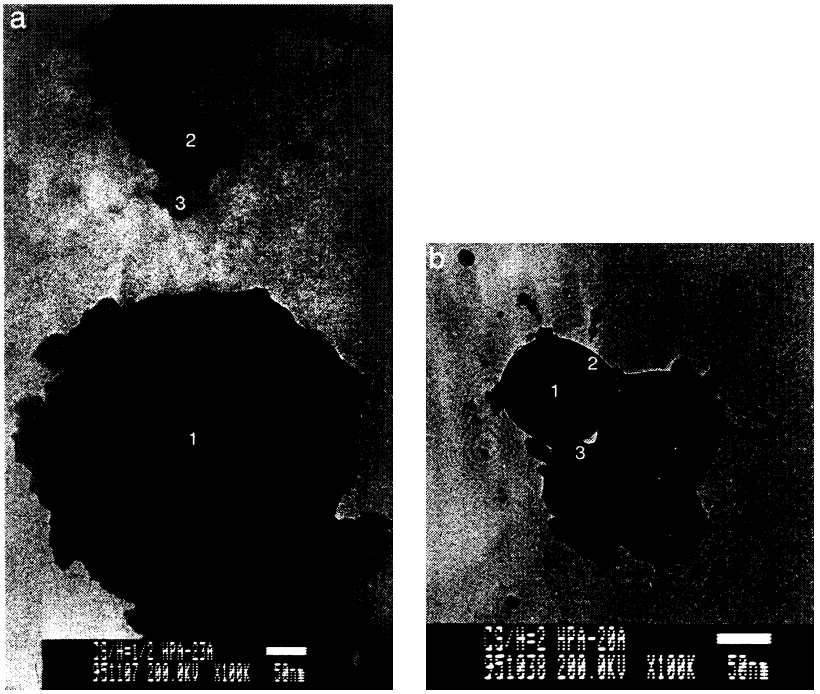

FIG. 7. Electron micrographs of particles of (a) Cs_1, (b) Cs_2. (The numbers correspond to EDX-STEM analyses with the results given in Table 4.)

but the selectivity to propene decreased significantly over the Cs salt. When the activity of the pure acid was examined it was seen to be comparable to the activity of the Cs_1H_2.

The study of the iron and copper substituted compounds in the isopropyl decomposition reaction was performed under nitrogen and the data obtained have been compared to those obtained with Cs_2H_1 tested under the same conditions (Table 8). The results showed that the decomposition activity went through a maximum with increasing copper content and the maximum took place at a copper content of 0.2 cation per KU. The product distribution changed in favor of DIPE and at the expense of propylene with increasing copper content. The selectivity for acetone remained unchanged around 3–4%. When conversion rates were compared for iron-containing compounds, a decrease was observed with increasing iron content up to a level of 0.2 cation per KU. Additional increase in iron content did not change the conversion rate. The product distribution did not vary significantly with iron content, with propene being the major product in all cases.

TABLE 7

Formation Rates and Selectivities Obtained in the Isopropyl Alcohol Decomposition in Air for the Undoped Cs_xH_{3-x} Compounds

Compound	Rate of propene formation (10^{-9} mol · $m^{-2} \cdot s^{-1}$)	Rate of propene formation (10^{-7} mol · $g^{-1} \cdot s^{-1}$)[a]	Selectivities (%) PRO	ACE	DIPE
		At 373 K			
Cs_1H_2	826	13.50	72	5	23
Cs_2H_1	90	24.38	72	6	22
$Cs_{2.5}H_{0.5}$	50	85.69	82	5	12
Cs_3	1	18.18	55	14	31
		At 353 K			
Cs_1H_2	351	5.71	77	3	20
Cs_2H_1	18	5.83	80	3	17
$Cs_{2.5}H_{0.5}$	12	19.54	85	2	13
Cs_3	0.15	2.72	62	6	31

[a] Rate expressed as mol/(g of acid phase · s).

TABLE 8

Formation Rate and Selectivities Obtained in the Isopropyl Alcohol Decomposition in Nitrogen for the Copper and Iron Doped Cs_2M_x Compounds

Compound	Rate of propene formation (10^{-9}mol · $m^{-2} \cdot s^{1}$)	Selectivities (%) PRO	ACE	DIPE
	At 373 K			
Cs_2H_1	50	75	3	22
$Cs_2Cu_{0.05}$	60	77	4	19
$Cs_2Cu_{0.2}$	67	74	3	22
$Cs_2Cu_{0.3}$	39	70	3	27
$Cs_2Cu_{0.43}$	29	67	4	29
Cs_2H_1	50	75	3	22
$Cs_2Fe_{0.1}$	36	70	5	25
$Cs_2Fe_{0.2}$	18	71	5	25
$Cs_2Fe_{0.25}$	18	72	3	25
$Cs_2Fe_{0.3}$	21	77	<1	22

DISCUSSION

The characterization of the solids of the type $Cs_xH_{3-x}PMo_{12}O_{40}$ with $0 < x < 3$, calcined at 623 K, showed that the compounds were composed of two phases: the cesium salt $Cs_3PMo_{12}O_{40}$ and the acid hydrated with 13 water molecules $H_3PMo_{12}O_{40} \cdot 13H_2O$, as proposed by Black *et al.* (11). These two phases were clearly identified in the samples by X-ray diffraction when the cesium content is low ($Cs < 2$), but at higher cesium contents only the peaks corresponding to the cesium salt were observed. Based on this observation, it was suggested that the salt containing at least two Cs atoms per KU might correspond to a solid solution and not to two distinct phases (12). Raman spectroscopy data appeared to be of particular interest for the characterization of the solids since it allowed the identification of both the salt and the acid phases over the entire composition range. As mentioned above, two bands at 1002 and 1009 cm^{-1}, attributed to the $\nu_s Mo{=}O_t$ vibration in the acid phase, have been observed in all the spectra, even in the so-called Cs_3 compound which contained a small amount of protons. Moreover, these two bands can be used as a measure of the degree of hydration of the acid since the spectrum of dehydrated acid showed mainly the band at 1009 cm^{-1}, whereas that of the hydrated acid exhibited the band at 1002 cm^{-1}. Nevertheless, the possibility of rehydration while recording the spectrum in air or dehydration by the laser beam did not allow for the assignment of the bands to a defined degree of hydration. In Fig. 8, we have plotted the integrated intensity of the two bands relative to the total intensity of the bands corresponding to the $\nu_s Mo{=}O_t$ vibration in different Cs_xH_{3-x} compounds (e.g., $(I_{1009} + I_{1002})/((I_{1009} + I_{1002} + I_{991} + I_{984})$ for $Cs_{1.5}H_{1.5}$). This intensity varied linearly with the cesium content, indicating that the technique may be used to determine the acid phase content of a given sample.

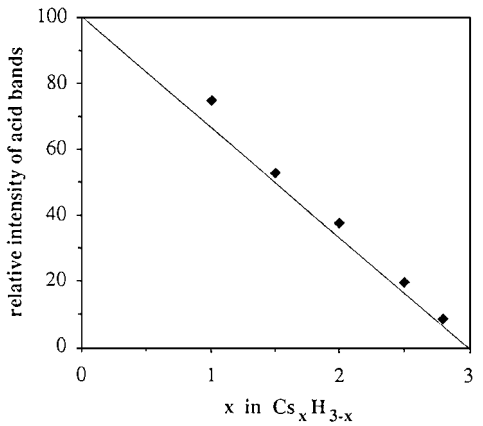

FIG. 8. Variation of the relative intensity of the Raman bands corresponding to the $\nu_s Mo{=}O_t$ vibration in the acid phase as a function of the cesium content in the Cs_xH_{3-x} compounds.

Electron microscopy studies provided additional support to the observations made through Raman spectroscopy. At low cesium content ($Cs = 1$), a bulk acid phase was observed coating the cesium particles. At higher cesium content ($Cs = 2$), a surface layer with a lower cesium content than the entire particle was observed, corresponding to a thin acid phase supported on the cesium salt. This supported phase seemed to be too thin to show a clear difference in contrast as in the case of the bulk acid in the sample Cs_1H_2. XPS data, showing less cesium at the surface than in the bulk, also confirmed the presence of the acid phase at the surface. When the results from different techniques are combined, they suggest that the compounds with a cesium content lower than 2 consist of cesium particles embedded-phase-supported on the cesium salt. This supported phase seemed to be too thin to show a clear difference in contrast as in the case of the bulk acid in the sample Cs_1H_2. XPS data, showing less cesium at the surface than in the bulk also confirmed the presence of the acid phase at the surface. When the results from different techniques are combined, they suggest that the compounds with a cesium content lower than 2 consist of cesium particles embedded in a bulk-acid phase, whereas at higher cesium contents, each cesium salt particle appears to be coated with a very thin film of the acid. This could explain both why the surface areas of the solids increased significantly above a cesium content of 2 and why the acid phase could not be detected by X-ray diffraction. It is also possible that the structure of this surface acid phase did not have a long-range order.

The TG analyses of the solids revealed a lower degree of hydration for the supported acid than for the bulk acid with 6–7 water molecules per KU, instead of 13. However, the Raman spectra showed the dehydrated acid to exist mainly in the solid containing a bulk-acid phase. This may indicate a greater stability of the supported acid against dehydration, as was also shown in TG analyses. Finally DTA data revealed no evidence for a change of stability of the acid by being supported on the cesium salt, since the exothermic peak of the MoO_3 formation did not shift in temperature for the different solids.

The substitution of protons by iron or copper did not modify the microstructure of the solids, even at high replacement levels. Raman spectra of the iron compounds were similar to those of the undoped compounds. The intensity of the bands at 1009 and 1002 cm^{-1} relative to the total intensity of the $\nu_s Mo{=}O_t$ vibration bands always varied linearly with the cesium content. No new phases were observed in XRD spectra. Electron microscopy/X-ray analysis indicated that the Keggin unit was intact in all samples by systematically showing a Mo/P ratio of 12. These results lead us to suggest that the transition metal cations occupied countercation positions in the heteropolycompound and no iron oxide, copper oxide, or molybdate phases were formed, even in small amounts. Moreover, the different techniques

used showed that the transition metal cation was in the acid phase, regardless of whether it was bulk or supported and not in the cesium salt. The substitution of iron, in our case, did acid. Nevertheless TG data revealed a higher stability of the hydrated state with the loss of the last five water molecules taking place at higher temperature (523 K). The hydrated form of the doped acid supported on the surface of the salt was observed to show the same higher stability, but a comparison of the doped and undoped supported acids revealed a reduced degree of hydration for the former.

We have confirmed that, depending upon the conditions of drying, the phosphomolybdic acid could be stabilized with only eight water molecules. Such an observation was also made for Cs_1H_2 compounds which contained a bulk acid phase. The 8-water-molecule hydrate seemed to show the same X-ray diffraction pattern as the triclinic phase with 13 water molecules with only an increased intensity of the peaks corresponding to the (0, k, −k) family of planes. It is conceivable that the loss of five water molecules does not involve a complete change of the structure but leads to a preferential orientation in favor of the of (0, k, −k) planes. From the structure determination, it has been shown that 8 of the 13 water molecules of the hydrated acid were involved in the formation of di- and tri-aquahydrogen ions (i.e., two water molecules in $H_5O_2^+$ ions and three in $H_7O_3^+$ ions) (20). It is, therefore, conceivable that the heteropolyacid with 8 H_2O molecules corresponds to the acid containing only the water molecules involved in the aquahydrogen ions, which interact with the polyanion oxygen atoms. However, it should be mentioned that the theoretical X-ray diffraction powder pattern of the acid calculated, taking into account only these water molecules, was practically the same as that calculated, taking into account all of the water molecules (28).

The results of the isopropyl alcohol decomposition on the Cs_xH_{3-x} compounds revealed that the acid phase is the catalytically active phase and confirmed that the pure cesium salt is practically inactive (29). It should be noted that our Cs_3 compound contained a small amount of acid as shown by chemical analysis (Table 1) and confirmed by Raman spectroscopy. This explains why the catalytic behavior obtained was somewhat comparable to those of the other compounds, even though the activity was very low. A comparison of the rates of product formation showed differences in activity, depending upon whether the acid phase was supported or not. A particular feature is the difference in activity between the compounds Cs_1H_2 and Cs_2H_1, the former being 10 times more active than the latter. This change was too significant to be simply related to a surface-type reaction since both solids showed an acid phase at the surface. This leads us to suggest that both the surface and the bulk of the acid should participate in the reaction in the case of Cs_1H_2. Such participation of the entire volume in the transformation of alcohols has already been demonstrated on heteropolyacids (30). These solids absorb polar reactant molecules like isopropyl alcohol and the reaction can take place in the entire volume with the rate being, thus, proportional to the volume of the active phase. The surface reaction appeared, however, predominant when the acid is supported as in Cs_2H_1 or $Cs_{2.5}H_{0.5}$. The strong interaction between the acid phase and the salt should limit the absorption of the alcohol possibly by limiting the expansion of the acid phase lattice. We have calculated the formation rates of propene per protons for Cs_1H_2, taking into account all the protons of the bulk (3 per KU), and for Cs_2H_1, taking into account only the protons at the surface with 1.5 protons per KU. These rates appeared to be comparable with 12.4×10^{-28} mol · s^{-1} per proton in the first case and 13.5×10^{-28} mol · s^{-1} per proton in the second. This seems to suggest that the acid is the active phase, regardless of whether the reaction is limited to the surface only (Cs_2H_1) or it takes place in the bulk as well (Cs_1H_2). The lower conversion rates of $Cs_{2.5}H_{0.5}$, compared to Cs_2H_1 may be explained by an incomplete coverage of the salt surface. Since the activity of the pure Cs salt is almost negligible, one would expect a reduction in activity as more salt is exposed on the surface. Finally, it should be noted that the activity of the Cs_2H_1 and $Cs_{2.5}H_{0.5}$ compounds, in which the acid was supported over the cesium salt, were comparable to that of the same acid supported on other supports such as zirconia or HMS (31).

It has been proposed that in the transformation of ethanol on Keggin-type heteropolyacids, the alkene was formed over the acid volume, whereas the ether was formed on acid sites at the surface (30). From our data obtained in the decomposition of isopropyl alcohol, it is difficult to make such a distinction between the propene and DIPE formation. The product distribution trends give no indication of a preferential formation of DIPE on the surface, leading us to suggest that both the alkene and the ether form indiscriminately in the bulk and on the surface.

The acidity of the compounds was also affected by the substitution of iron and copper cations in the supported acid phase. Since the transition metal countercations replace the protons in the acid phase and not the cesium cations, its presence should lead to the same amount of the acid phase, only less rich in protons. The decrease in the number of protons should thus decrease the acidity of the solids. The fact that copper substitution increased the rate of propene formation up to a composition of $Cs_2Cu_{0.2}$ suggests that the acid sites formed by copper were more active than the replaced protons. Nevertheless, at higher copper contents the activity decreased, showing that the additional copper has no beneficial effect on the acidity. In the case of iron substitution, the linear decrease of acidity up to the composition of $Cs_2Fe_{0.2}$ is proportional to the loss of protons. Iron has thus no specific effect on the acidity at low contents. At higher cation content the acidity of the compounds

remained constant, which is difficult to explain. It is possible that at high content levels, iron could partially be present as $[Fe(OH)_x]^{(3-x)+}$ species which would act as active sites and compensate for the loss of activity due to the decrease in the number of protons. It has been proposed that in mixed ammonium and potassium salts and at higher contents, iron could form such species as countercations (9). Moreover, it has been reported that in this case iron had a positive effect on the acidity of the compounds (9).

CONCLUSIONS

The results obtained from different characterization techniques used in this study lead us to conclude that the cesium substituted heteropolycompounds are comprised of two phases which correspond to the acid and the cesium salt. It is conceivable that during the preparation, the cesium salt is precipitating first and that the acid is covering the salt particles. Our results confirm the proposition of Black *et al.* (10) who previously proposed this microstructure in the case of potassium substituted heteropolycompounds. It has also been confirmed that, depending upon the conditions of drying, the acid which generally crystallized with 13–14 H_2O molecules, could be stabilized with only 8 H_2O molecules. In this last case the partial dehydration seems not to induce a change of the structure, but only a preferential orientation with the development of the (0, k, −k) planes. It is possible that an interaction between the cesium salt as support and the supported acid plays a role in the stabilization of the acid phase in a less hydrated state.

Raman spectroscopy has been shown to be a very effective technique for characterization of the cesium-substituted heteropolyacids, allowing the identification of the acid and the salt phases even at low contents. This technique also allowed quantification of the acid phase loading in the compounds.

The isopropyl alcohol decomposition experiments showed a "bulk" activity of the acid through absorption of the alcohol in the acid phase. In the case of the supported acid, the interaction with the salt support appeared to limit its alcohol absorption properties.

When a transition metal cation is added as counter cation, it was found to preferentially substitute the protons in the acid phase. It had no effect on the structural characteristics of the acid, but appeared to affect its hydration activity. However, this effect was limited to the supported acid only. It was observed that copper increased the acidity up to a maximum corresponding to 0.2 transition metal cation per Keggin unit, whereas iron decreased it.

Redox and catalytic properties of these cesium and transition metal-subsituted heteropoply compounds in isobutane oxidation are presented in the second article of this series (32).

REFERENCES

1. Mizuno, N., and Misono, M., *Current Opinion in Solid State & Materials Sci.* **2**(1), 84 (1997).
2. Moffat, J. B., *Appl. Catal. A* **146**(1), 65 (1996).
3. Albonetti, S., Cavani, F., Trifiro, F., and Koutyrev, M., *Catal. Lett.* **30**, 253 (1995).
4. Cavani, F., Koutyrev, M., and Trifiro, F., *Catal. Today* **28**, 319 (1996).
5. Mizuno, N., Tateishi, M., and Iwantoto, M., *Appl. Catal. A* **128**, L165 (1995).
6. Ai, M., *in* "Proc. 8th Internat. Congr. Catal., 1984," Vol. V, p. 487.
7. Mizuno, N., Tateishi, M., and Iwamoto, M., *J. Chem. Soc. Chem. Commun.*, 1411 (1994).
8. Mizuno, N., Tateishi, M., and Iwamoto, M., *J. Catal.* **163**, 87 (1996).
9. Cavani, F., Etienne, E., Favaro, M., Galli, A., and Trifiro, F., *Catal. Lett.* **32**, 215 (1995).
10. Staroverova, I. N., Kutyrev, M., and Stakheev, A., *Kinet. i Katal.* **33**(1), 127 (1992).
11. Black, J. B., Clayden, N. J., Gai, P. L., Scott, J. D., Serwicka, E. M., and Goodenough, J. B., *J. Catal.* **106**, 1 (1987).
12. Okuhara, T., Nishimura, T., Watanabe, H., Na, K., and Misono, M., Acid-base catalysis II, *in* "Stud. Surf. Sci. Catal." (H. Hakori, M. Misoono, and Y. Ono, Eds.), Vol. 90, p. 419, Elsevier, Amsterdam, 1994.
13. Tsigdinos, G. A., *Ind. Eng. Chem., Prod. Res. Develop.* **13**, 267 (1974).
14. Mentzen, B. F., *J. Appl. Crystallogr.* **22**, 100 (1989).
15. Védrine, J. C., and Jugnet, Y., *in* "Les techniques physiques d'étude des catalyseurs" (B. Imelik and J. C. Védrine, Eds.), Chap. 10, p. 365, Technip, Paris, 1988.
16. Fournier, M., Feumi-Jantou, C., Rabia, C., Hervé, G., and Launay, S., *J. Mater. Chem.* **2**(9), 971 (1992).
17. Misono, M., Mizuno, N., and Komaya, T., *in* "Proceedings of the 8th International Congress on Catalysis," Vol. 5, p. 487, Verlag Chemie, Berlin, 1984.
18. McMonagle, J. B., and Moffat, J. B., *J. Colloid Interface Sci.* **101**, 479 (1984).
19. Hibi, T., Takahashi, K., Okuhara, T., Misono, M., and Yoneda, Y., *Appl. Catal.* **24**, 69 (1986).
20. Von d'Amour, H., and Allamnn, R., *Z. Krist.* **143**, 1 (1976).
21. Brown, G. M., Noe-Spirlet, M. R., Busing, W. R., and Levy, H. A., *Acta Cryst. B* **33**, 1038 (1977).
22. Mattes, R., Bierbusse, H., and Fuchs, J., *Z. Anorg. Allgem. Chem.* **385**, 230 (1971).
23. Rocchiccioli-Deltcheff, C., Thouvenot, R., and Franck, R., *Spectrochim. Acta A* **32**, 587 (1976).
24. Mc Carron, E., *J. Chem. Soc. Commun.*, 336 (1986).
25. Shimoda, T., Okuhara, T., and Misono, M., *Bull Chem. Soc. Jpn* **58**, 2163 (1985).
26. Coulston, G. W., Thompson, E. A., and Herron, N., *J. Catal.* **163**, 122 (1996).
27. Etienne, A., Ph.D. thesis, Lille, 1996.
28. Langpape, M., Ph.D. thesis, Lyon, 1997.
29. Chelighem, B., Ph.D. thesis, Paris VI, 1996.
30. Okuhara, T., Kasai, A., Hayakawa, N., Yoneda, Y., and Misono, M., *J. Catal.* **83**, 121 (1983).
31. Coudurier, G., private communication, 1997.
32. Langpape, M., Millet, J. M. M., Ozkan, U. S., and Delichère, P., *J. Catal.*, in press.